Atefe Atarodi[1]
Mahmoud Chamsaz[1]
Ali Zeraatkar Moghaddam[2]
Hadi Tabani[3]

[1]Department of Chemistry, Faculty of Sciences, Ferdowsi University of Mashhad, Mashhad, Iran
[2]Department of Chemistry, Faculty of Sciences, University of Birjand, Birjand, Iran
[3]Department of Environmental Geology, Research Institute of Applied Sciences (ACECR), Shahid Beheshti University, Tehran, Iran

Received January 4, 2016
Revised January 25, 2016
Accepted January 25, 2016

Research Article

Introduction of high nitrogen doped graphene as a new cationic carrier in electromembrane extraction

This paper proposes for the first time, the use of high nitrogen doped graphene (HND-G) as a new cationic carrier for the enhancement of electromembrane extraction (EME) performance. Sensitivity of EME was improved by the modification of supported liquid membrane composition through the addition of HND-G into 1-octanol for the extraction of naproxen and sodium diclofenac as model acidic drugs. The comparison between HND-G-modified EME and conventional EME showed that HND-G could increase the overall partition coefficient of acidic drugs in the membrane due to the fact that HND-G acts as an ion pair reagent and there is an electrostatic interaction between positively charged HND-G and acidic drugs with negative charge. During the extraction, model acidic drugs migrated from a 10 mL aqueous sample solution (pH 9.6) through a thin layer of 1-octanol containing 0.6% w/v of HND-G that was impregnated in the pores of a hollow fiber, into a 30 μL basic aqueous acceptor solution (pH 12.3) present in the lumen of the hollow fiber. Equilibrium extraction conditions were obtained after 16 min of operation with the whole assembly agitated at 1000 rpm. Under the optimized conditions, the enrichment factors were between 238 and 322 and also the LODs ranged from 0.1 to 0.7 ng/mL in different samples. Finally, the applicability of this method was evaluated by the extraction and determination of drugs of interest in real urine samples.

Keywords:
Box–Behnken design / Electromembrane extraction / High nitrogen doped graphene / Modified supported liquid membrane DOI 10.1002/elps.201600001

Additional supporting information may be found in the online version of this article at the publisher's web-site

1 Introduction

Hollow fiber based liquid-phase microextraction (LPME), in which organic solvents of low polarity are immobilized as a thin liquid membrane in the wall of a hollow fiber, benefits from very low consumption of organic solvents and it can be operated in a three-phase mode where the final extract is an aqueous solution that is directly compatible with LC [1–4]. The extraction depends both on the distribution constants among the aqueous sample, supported liquid membrane (SLM), and the acceptor solution. The difference in optimal pH values on both sides of the SLM encourages mass transfer. For extraction of basic compounds, pH in the donor phase (DP) should be adjusted into the alkaline region to suppress analyte solubility, whereas pH in the acceptor phase (AP) should be low in order to promote analyte solubility. In this manner, the basic compounds may be easily extracted into the organic phase and further into the AP. By contrast, for acidic analytes, pH in the DP should be low and an alkaline AP should be utilized within the lumen of the fiber [5]. In addition, extraction could be further promoted by strong agitation of the extraction system, which reduces the stagnant boundary layer in the vicinity of the SLM-inducing convection in the sample. However, even in the optimized conditions, LPME is a relatively time-consuming process and extraction times within the range of 30–90 min are common. Electrokinetic transport

Correspondence: Professor Mahmoud Chamsaz, Department of Chemistry, Faculty of Sciences, Ferdowsi University of Mashhad, Mashhad, Iran
Fax: 0098915-315-5115
E-mail: mchamsaz@gmail.com

Abbreviations: **AP**, acceptor phase; **BBD**, Box–Behnken design; **DP**, donor phase; **EF**, enrichment factorEME electromembrane extraction; **G**, graphene; **GO**, graphene oxide; **HND-G**, high nitrogen doped graphene; **NAP**, naproxen; **ND-G**, nitrogen doped graphene; **SDF**, sodium diclofenac; **SLM**, supported liquid membrane; **XPS**, X-ray photoelectron spectroscopy

Colour Online: See the article online to view Figs. 2-3 in colour.

by applying two electrodes, one in the donor aqueous sample and the other in the aqueous acceptor solution and an electrical potential difference between them, can overcome this major drawback in the extraction time [1–5]. This new concept is called electromembrane extraction (EME) that has been used for the extraction of several basic and acidic drugs with different log *P* values from biological and environmental samples [6–16]. Charged analytes in the DP migrate across the SLM, toward the electrode of opposite charge in the AP.

Optimization of the chemical composition of SLM is a main part of the EME procedure. Because this parameter affects the efficiency and the selectivity of the system. Based on earlier finding, basic analytes were successfully extracted with nitro aromatic solvents such as NPOE [4] Also, it has been found that the addition of hydrophobic ion-pair reagents such as di-(2-ethylhexyl) phosphate or tri-(2-ethylhexyl) phosphate to SLM could improve phase transfer and electrokinetic migration of basic analytes with low polarity [4]. On the other hand, 1-octanol and 1-octanol plus some CTAB, an ion-pairing agent, have been used for the extraction of acidic drugs of higher and lower hydrophilicity, respectively [12, 16]. In another report, Ramos-Payan et al. [17] introduced a new modified membrane to EME procedure. Silver nanoparticles were dispersed into the SLM and it was used for the extraction of nonsteroidal anti-inflammatory drugs. This new membrane caused an increase in the electrokinetic migration across the SLM. Another important modification on EME procedure was the introduction of ionic liquids as the SLM. Sun et al. reported the extraction of basic drugs using an ionic liquid ([C6MIm][PF6]) as the SLM [18]. Slampova et al. reported the application of crown ethers in the SLM for the extraction of potassium ions. An SLM containing 1% w/v of dibenzo-18-crown-6 in NPOE exhibited good selectivity of EME for K^+. The established host–guest interactions between crown ether cavities in the SLM and potassium ions in the DP ensured their almost exhaustive transfer into the AP within 30 min of EME at 50 V [19]. Following the improvement of the EME technique, the use of multiwalled carbon nanotubes in EME was reported by Hasheminasab et al. [20, 21]. The multiwalled carbon nanotubes dispersion in the SLM allows an additional adsorption/desorption process beside the electrokinetic transportation from the DP to the AP. The presence of the nanotubes caused a larger surface area, and also contributed to increase the overall analyte partition and transportation of the compounds across the membrane.

Another carbon nanostructured material that can be immobilized in the SLM is graphene (G). G is a type of carbon with a one-atom thick two-dimensional (2D) layer of sp^2 bonded that was firstly described in 2004 [22], and has found its way to material science due to its special properties [22]. It has a large surface area and high electrical conductivity in comparison with the other types of carbon such as CNTs. The electronic and chemical characteristics of G have been studied by scientists. The main drawback of G nanostructures is the low dispersibility in organic solvent such as 1-octanol, which can cause the accumulation of these materials and the blockage of hollow fiber pores. Plus the fact that there is not any suitable function group on the G for a proper interaction with anionic analytes. Thus in this study, G nanostructures were doped with various amounts of nitrogen (N). In general, chemical doping with N is considered as an effective method to intrinsically modify the properties of carbon materials. Nitrogen has a proper size as well as five valence electrons and creates powerful bonds with carbon atoms so it is considered as a good dopant [23]. Another distinct property of G is that it makes higher positive charge on a carbon atom closed to the nitrogen atoms [24], which cause nitrogen doped graphene (ND-G) to form ion-pair with analytes that possess negative charge. The resulting ion-pair is soluble in liquid membrane enhancing the extraction efficiency. Also, the introduction of N groups into G nanoparticles improves the dispersibility of these materials and the electrostatic repulsion caused by N group prevents any aggregation [25].

Recently, ND-CNTs were used to increase the extraction efficiency in solid-phase microextraction [26], but to our best of knowledge there has not been any report in the application of these materials in EME technique. Thus, in this study, N-doped G nanoparticles were synthesized with different percentages of N and were added into the SLM as cationic carriers and subsequently the extraction efficiency of modified EME for sodium diclofenac (SDF) and naproxen (NAP) as model acidic drugs was investigated. To define the optimum values of effective parameters on extraction efficiency, the response surface plots were depicted from the model obtained by Box–Behnken design (BBD). Ultimately, due to the importance of analyzing the drugs in biological samples, final experiments were carried out on three real urine samples.

2 Materials and methods

2.1 Chemicals and materials

SDF (purity >99.0%) and NAP (purity >99.0%) were supplied by Daroupakhsh Pharmaceutical Company (Tehran, Iran) and were used without any further purification. All the analytical grade solvents including methanol, acetone, acetonitrile, and 1-octanol were purchased from Merck (Darmstadt, Germany). $KMnO_4$, $K_2S_2O_8$, P_2O_5, H_2O_2, H_2SO_4, HCl, NaOH, urea, hydrazine hydrate and ammonia were purchased from Fluka (Buchs, Switzerland). The G and graphene oxide (GO) were purchased from Research Institute of the Petroleum Industry (Tehran, Iran). HPLC grade water was obtained through a Milli-Q® system (Millipore, Milford, MA, USA) and was used to prepare all solutions.

2.2 Standard and real sample solutions

Stock solution of each drug (1000 mg/L) was prepared in HPLC grade water. The stock solutions were protected from light and stored for 1 month at 4°C with no evidence of decomposition. All required standard solutions were prepared daily from these stock solutions and were diluted with

HPLC grade water. The pH values of all AP and DP solutions were adjusted by dropwise addition of 1 M of NaOH solution.

The real urine samples were obtained from Taleghani Hospital (Tehran, Iran). The samples were stored at −4°C, thawed, and shaken before extraction. Urine 1 sample was collected from a volunteer who had not consumed SDF and NAP at all. Urine samples 2 and 3 were taken from patients who were under treatment with SDF (100 mg/day) and NAP (500 mg/day), after 6 h and 150 min from oral administration of tablets, respectively. The urine samples were diluted at 1:1 ratio using HPLC grade water and their pH values were adjusted at 9.6 with the addition of 1 M of NaOH solution.

2.3 Apparatus

X-ray photoelectron spectroscopy (XPS) analysis was performed using a Gammadata-scienta ESCA 200 hemispherical analyzer equipped with an Al Ka (1486.6 eV) X-ray source. The FT-IR measurements were carried out using a Bomem MB Series FT-IR spectrometer in the form of KBr pellets. Raman spectra of nanostructures were recorded on a Bruker SENTERR (2009) with an excitation beam wavelength at 785 nm. The CHNS analysis was performed on a Thermo Finnigan Flash EA112 elemental analyzer (Okehampton, UK). Ultrasonic bath (Eurosonic 4D ultrasonic cleaner with a frequency of 50 kHz and an output power of 350 W) was used to disperse materials in organic solvent.

Separation, identification, and quantification of the drugs were carried out on a HPLC from Shimadzu company (Tokyo, Japan) equipped with a binary solvent delivery pump, a SPD-10 AV UV–Vis detector and a manual injector. SDF and NAP were separated on a Knauer C18 (150 × 4.6 mm; 5 μm) column. The mobile phase consisted of phosphate buffer (pH 3.2; component A) and methanol (component B). Component A was prepared by mixing equal volumes of 0.01 M phosphoric acid with 0.01 M sodium dihydrogen phosphate. The LC program was the isocratic elution with 40% of component A and 60% of component B at a flow rate of 1 mL/min The wavelength used for the UV detector was 280 nm [27].

2.4 Preparation of high nitrogen doped graphene (HND-G) and ND-G

Preparation of high nitrogen doped graphene (HND-G) and ND-G were carried out based on the method reported by Movahed et al. [28]. In brief, a solution containing 140 mg GO dispersed in 70 mL distilled water was applied and the pH of this sample was adjusted at 10 using ammonia 30%. Then, 2 mL of hydrazine hydrate was added while stirring magnetically for 10 min. After that, the solution was sealed in a 50 mL Teflon-lined autoclave and maintained at 80°C for 3 h. The reduced G sheets were collected with centrifugation, followed by washing several times with deionized water and were then dried in vacuum oven at 50°C.

For the preparation of HND-G, a solution containing 40 mg GO dispersed in 10 mL distilled water was prepared and then diluted with 25 mL of deionized water. Then the mixture was sonicated for about 3 h and 12 mg of urea was added to the sample solution simultaneously. After that, the solution was sealed in a 50 mL Teflon-lined autoclave and maintained at 180°C for 12 h. The solids (HND-G) were filtered and washed several times with distilled water. Finally, the HND-G was collected and dried in a vacuum oven at 80°C.

2.5 Electromembrane equipment and extraction procedure

The DC power supply used was a model PV-300 (Mobtaker Aryaei J., Zanjan, Iran) with programmable voltage in the range of 0–300 V, providing currents in the range of 0–1.0 mA. Two platinum wires of 0.2 mm diameter were used as the electrodes (one electrode served as cathode and *the other one as anode*) with 5 mm interelectrode distance between them in a sample vial, and they were connected to the power supply. The porous hollow fiber used for the immobilization of the SLM and housing the AP was a PP Q3/2 polypropylene hollow fiber (Membrana, Wuppertal, Germany) with an internal diameter of 1.2 mm, a 200 μm wall thickness, and 0.2 μm pores. It was cut into 3.5 cm segments, cleaned in acetone, and dried prior to use. Stirring the solutions was carried out by a Heidolph MR 3001 K magnetic stirrer (Schwabach, Germany) using 1.5 × 8 mm magnetic bars.

In order to immobilize ND-G and HND-G into the wall pores of hollow fiber, each one of these carbon nanostructures was separately dispersed in 1-octanol and then the mixture was gradually injected into the hollow fiber manually using an HPLC syringe and it was sonicated for 15 min. After that, carbon nanostructures reinforced hollow fibers were washed with 1-octanol several times to remove the excess nanostructured materials from the surface and the inner lumen of the fiber, until no carbon nanostructures were observed in the washing solvent.

A 10 mL sample solution (pH 9.6) was filled into a glass vial. After the impregnation of hollow fibers with carbon nanostructures, the lumen of the hollow fibers was filled with 30 μL of basic aqueous solution (pH 12.3) as an anodic AP using a microsyringe and the end of the hollow fibers were sealed with a pair of hot flat-tip pliers. The fiber containing the anode, the SLM (organic solvent along with carbon nanostructures) and the AP was simultaneously introduced into the sample solution. The electrodes were subsequently coupled to the power supply and the sample vial was placed on a stirrer at a stirring rate of 1000 rpm. A 68 V DC potential was applied between the anode and cathode for 16 min. Finally, the power supply was turned off and the hollow fiber was taken out from the DP. The sealed end of the hollow fiber was cut with scissors, and the AP was collected by a microsyringe and then injected to HPLC for further analysis.

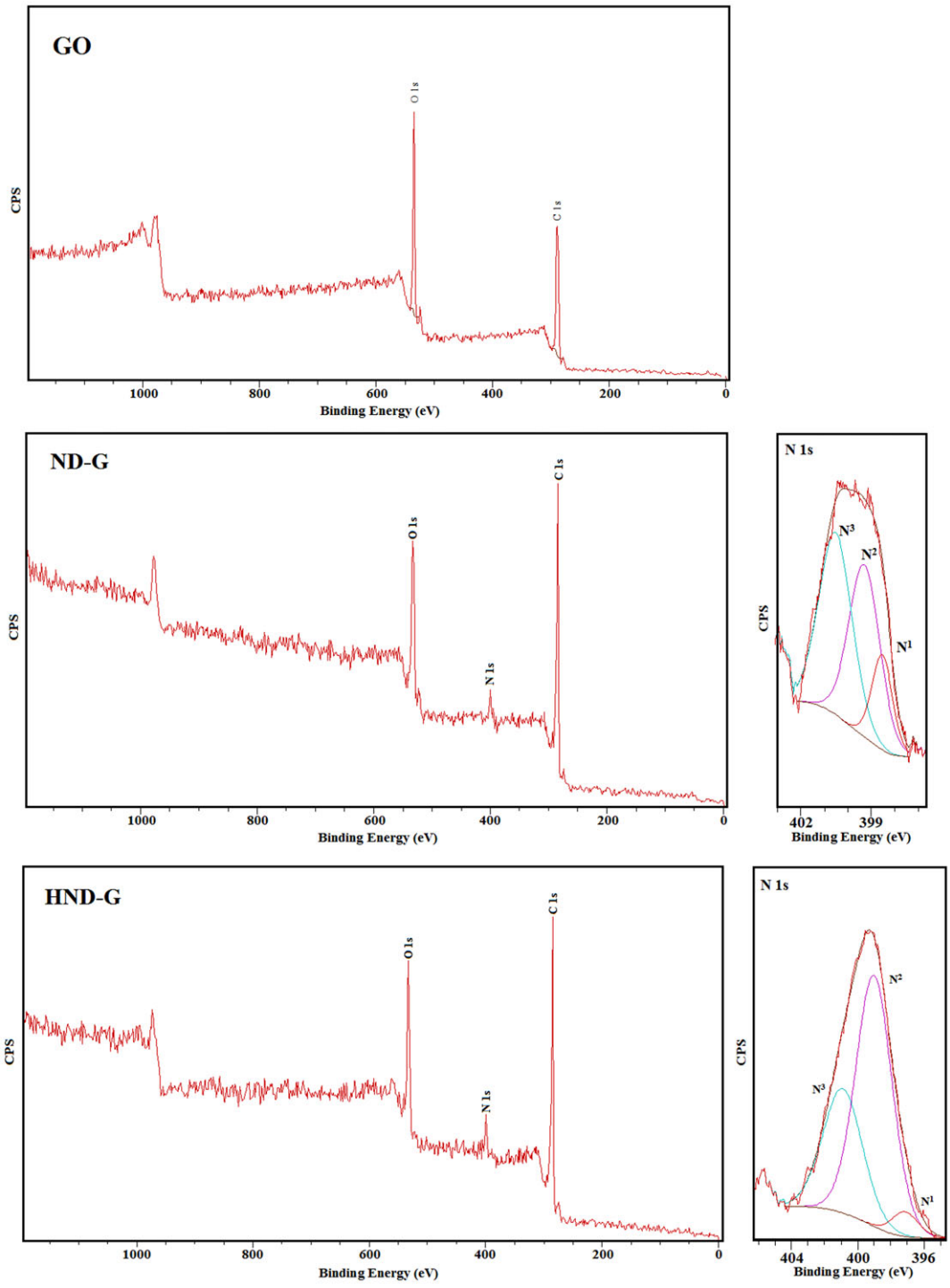

Figure 1. Full-range XPS spectra of ND-G, and HND-G composites and related N 1s core-level region.

3 Results and discussion

3.1 Characterization of ND-G and HND-G

XPS, a powerful tool to identify the elements' states in bulk material, was used to prove the existence of different types of nitrogen in the structure of G [29]. The XPS survey spectra of GO, ND-G, and HND-G indicated the presence a C ((1)s) peak at 285.3 eV and an O ((1)s) peak that is appeared at 532.5 eV (Fig. 1). In addition, ND-G and HND-G have an N ((1)s) peak at 399.4 eV that this peak is related to presence of nitrogen in their structures. Also, from the N 1s XPS scan

Table 1. The nitrogen, carbon, hydrogen content of GO, ND-G, and HND-G

Entry	N content (%)	C content (%)	H content (%)	N/C
GO	0	71.28	0.9	—
ND-G	3.19	70.25	1.39	0.04
HND-G	11.24	65.81	2.03	0.17

shown in Fig. 1, it is observed that the N 1s peak can be split to three individual peaks at 398, 399, and 401 eV, which are assigned to pyridinic N (N^1), pyrrolic N (N^2), and graphitic N (N^3), respectively [30, 31]. Thus, it is clear that nitrogen was doped into the G structure.

Raman spectroscopy is a very useful and nondestructive tool to identify the quality and the doping effect of G [32]. The Raman spectra of prepared GO, ND-G, and HND-G are shown in Supporting Information Fig. 1. The characteristic D and G bands of carbon materials are observed at around 1285 and 1570 cm^{-1}, respectively. The D band is usually related to a series of defects, including bonding disorders and vacancies in G lattice induced by nitrogen doping and it is characteristic of a breathing mode for k-point phonons of A_1g [33]. The G band, is commonly observed for all graphitic structures and can be attributed to the E_{2g} vibrational mode present in the sp^2-bonded graphitic carbons [33]. The D bands are significantly enhanced in ND-G and HND-G in comparison with GO since pyridinic and pyrrolic nitrogens are accompanied by defects inside the G network and by the functional edges of G sheets (Supporting Information Fig. 1). The G bands of ND-G and HND-G -G shift to higher frequencies (9.94 and 8.77 cm^{-1}, respectively) with respect to that of GO. The intensity ratio of D band to G band, namely the I_D/I_G ratio, provides the gauge for the amount of structural defects and a quantitative measure of edge plane exposure [34]. As shown in Supporting Information Fig. 1, after the introduction of N on GO sheets, the I_D/I_G were 1.57, and 1.78 for the resulting ND-G and HND-G, respectively, while the I_D/I_G of GO was 1.49. The higher I_D/I_G ratio for ND-G and HND-G is a result of the structural defects and edge plane exposure caused by heterogeneous nitrogen atom incorporation into the G layers [35].

Furthermore, FT-IR spectra were used to investigate the bonding difference between HND-G, ND-G, and GO (Supporting Information Fig. 2). The peak intensity of carbonyl (C = O) at 1722 cm^{-1} of the HND-G and ND-G obviously decreases, compared to that of GO. Also, a new peak is certainly identified at about 1550 cm^{-1} that can be assigned to sp^2 bonded C = N, demonstrating the formation of the C–N bond in HND-G and ND-G [36].

In order to obtain the amounts of N present in the structure of ND-G and HND-G, the CHNS analysis was done. The weight percentage of N, C, H, and N/C ratio of composites are shown in Table 1. As shown in Table 1, the atomic percent of N for ND-G and HND-G is 3.19 and 11.24%, respectively, which confirms the successful synthesis of the mentioned nanostructures.

3.2 Optimization strategy

To obtain the maximum extraction recoveries for simultaneous extraction of NAP and SDF drugs, the effective parameters of EME including, the SLM composition, stirring rate, extraction time, applied voltage, salt addition (ionic strength), and pH of the donor and AP were investigated.

The effect of type and amount of carriers in the SLM on the extraction efficiency was evaluated using one variable at a time methodology. Then, the influence of the other factors (extraction time, applied voltage, and pH of the donor and APs), was evaluated by BBD methodology.

Among the impressive variables, stirring rate and organic solvent in the SLM were separately studied. According to the literature, for the extraction of acidic drugs the best analyte flux through the SLM is obtained using 1-octanol as the organic solvent in the SLM [37–39]. The high efficiency of 1-octanol is related to high Kamlet and Taft values for polarizability (π) and hydrogen bond acidity (α) [38]. Also, it was observed that formation of intense whirlpool in sample solution and bubble formation around the hollow fiber at the stirring rates higher than 1000 rpm significantly decrease the extractability [9,16]. Thus, the maximum stable rate (1000 rpm) was applied in all the experiments. Also according to the previous studies [8, 9, 11, 16], the presence of high content of ionic substances causes an increase in the value of the ion balance (χ), which is defined as the ratio of the total ionic concentration in the sample solution to that in the acceptor solution, which in turn decreases the flux of analytes across the SLM. Therefore, this factor was removed from variables.

3.2.1 The effect of type and concentration of carrier

For investigating the effect of the presence of G, GO, ND-G, and HND-G as carriers in the SLM, 0.5% of each was dispersed in 1-octanol separately, and extraction was carried out. The results (Fig. 2) revealed that ND-G and HND-G can act as the best carriers due to the presence of N groups and higher dispersibility of these materials compared to that of G. The introduction of N groups into G nanoparticles improved the dispersibility of these materials due to the N containing hydrophilic part and also the electrostatic repulsion caused by N groups prevented further aggregation. In addition these materials have positive charge on a carbon atom closed to the nitrogen atoms [24], which itself causes HND-G to form ion-pair with acidic drugs that possess negative charge. This result can be concluded through the comparison of extraction efficiencies between HND-G with ND-G, so that HND-G that has 11.24% N in its structure showed higher extraction efficiencies in comparison with ND-G with 3.19% N. It is worth mentioning that, worse extraction efficiency of GO in comparison with G can be attributed to the fact that GO contains a number of functional groups, such as carboxylic acid and phenolic hydroxyl groups that in basic media are in the negative

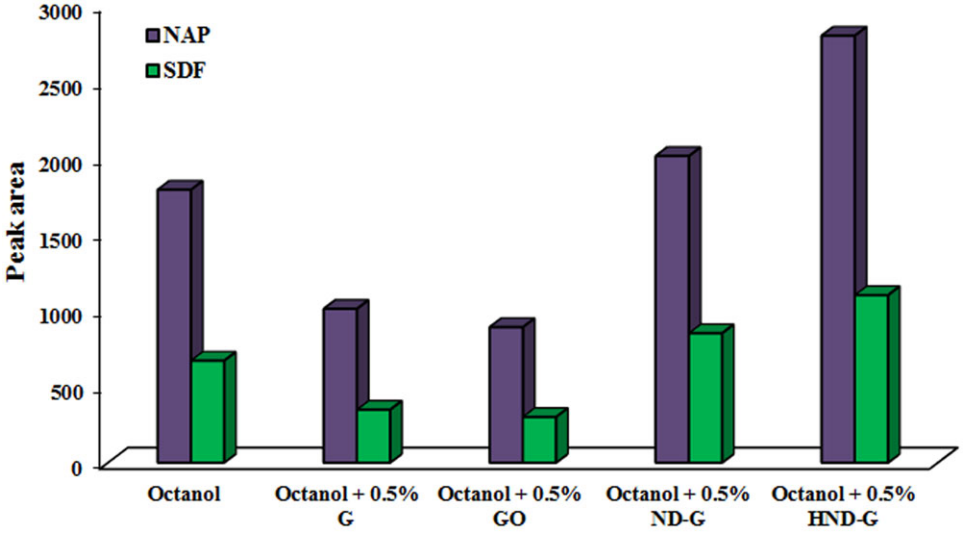

Figure 2. Influence of type of the carriers on the extraction efficiency. Concentration of each drug: 60 ng/mL, voltage: 40 V, pH of the DP: 8.0, pH of the AP: 12.0, extraction time: 20 min.

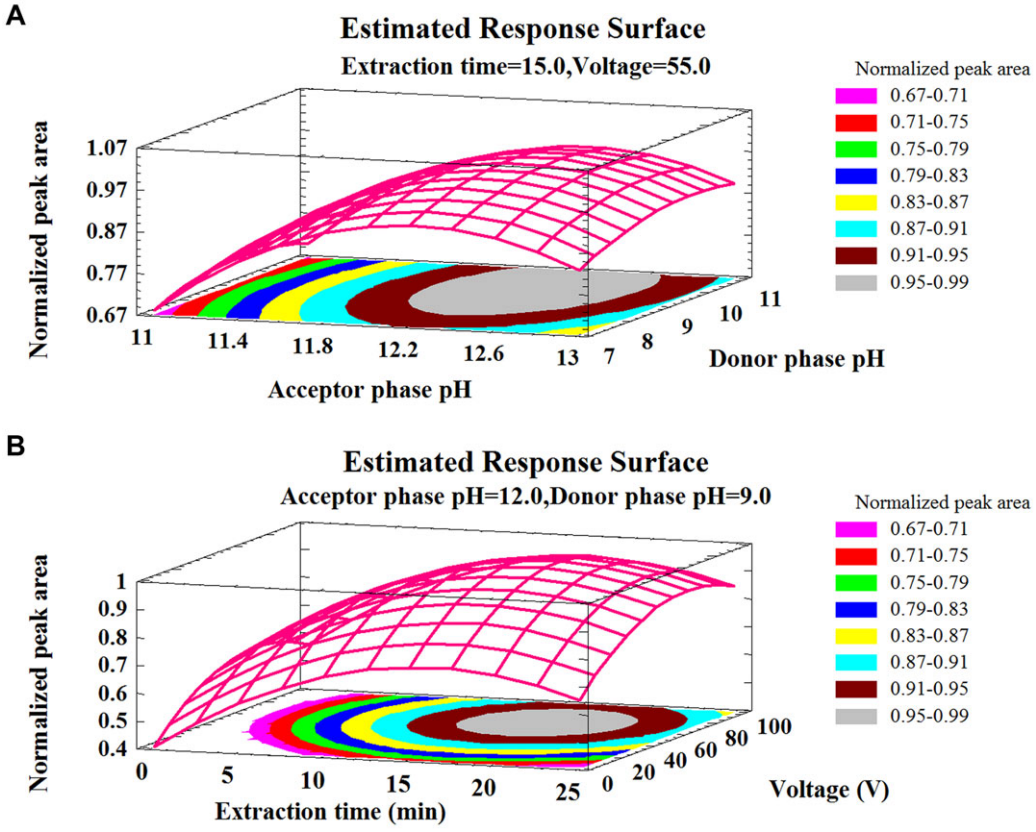

Figure 3. Response surface methodology and contour plots obtained by plotting of (A) pH of the DP versus pH of the AP, and (B) extraction time versus voltage, using the BBD.

forms [40] and, evidently, they have an electrostatic repulsion with anionic acidic drugs. Thus, HND-G was selected as the most appropriate carrier for the rest of the studies.

In the following optimization process, the effect of the HND-G concentration in 1-octanol on the extraction efficiency was examined in the range of 0.2–1% w/v. Supporting Information Fig. 3 indicates that signal intensities improved with increasing the concentration of HND-G up 0.6% w/v and after that, the recoveries decreased. It can be attributed to the fact that at high concentrations of HND-G, the strong interaction between the complex constituents (the ion-pair and the drugs) in the organic phase or accumulation of HND-G

in the pores that would block the pores of hollow fiber may be responsible for this behavior. Therefore, the best SLM composition for the extraction of these drugs was 0.6% HND-G in 1-octanol.

3.2.2 Optimization by BBD

The experiments for optimizing the rest of the EME-affecting parameters (extraction time, applied voltage and pH of the donor and AP) were modeled through BBD. BBD is a spherical, revolving design, it consists of a central point and the middle points of the edges of the cube circumscribed on the sphere [41]. This design is suitable for exploring quadratic response surface and constructing second-order polynominal models. Experimental data were fitted to a quadratic polynomial model and regression coefficients were obtained. The experimental design matrix and data analysis were performed by the Statgraphics Plus Package (version 5.1; Statistical Graphics, Manugistics, USA) [42]. The total number of experiments (N) was calculated as below:

$$N = 2k(k-1) + C_p$$

where k is the number of variables and C_p is the number of centre points [9]. Thus, this experimental design consists of 29 experiments with five center points (in order to allow the estimation of pure error) and allows the calculation of the response function at intermediate levels and enables the estimation of the system performance at any experimental point within the studied range. The examined levels of these factors are given in Supporting Information Table 1. These levels were selected based on previous works [9, 12, 13, 16]. The normalized peak area for each run was selected as the response objective for the study. To normalize the peak areas, all of the experiments were first conducted and then the peak area of each analyte was divided by its smallest peak area that was attained from the entire experiments.

The normalized peak area obtained was evaluated by the ANOVA, and the main effects were visualized by the use of a Pareto chart (Supporting Information Fig. 4). In the Pareto chart, the bar lengths are proportional to the absolute value of the estimated main effects. The chart also includes a vertical line corresponding to 90% confidence interval. An effect exceeding this reference line may be considered significant with regard to the response. Furthermore, the positive or negative sign (corresponding to a colored or colorless response) can enhance or reduce the response, respectively, when passing from the lowest to the highest level set for the specific factor. According to Supporting Information Fig. 4 four main factors and the interaction between some of them showed statistically significant effects at the $p < 0.05$ level. Also, this figure shows that pH of the AP has a large influence on the normalized peak area and a positive effect upon the extraction. Based on the extraction principles of EME, the AP should be strongly alkaline in order to ionize the analytes. The pH in the AP gradually decreased during the process due to electrolysis. In order to suppress this effect, a high initial pH value for AP was required [7]. Also, theoretical studies show that the total ionic concentration of the DP to that of the AP (χ), which is mainly determined by the pH of both phases, impresses the flux over the membrane and the flux may decrease as this ratio increases [8, 39]. Since there is an antagonistic effect among these parameters, they were simultaneously considered, and the interaction of the pH of the acceptor and DP was investigated using response surface methodology (Fig. 3A). Based on the analysis and plots presented in this figure, it can be observed that the normalized peak area of drugs increased in a quadratic manner with an increase in the pH value of the AP while the pH of the DP showed a nonsignificant effect on the extraction efficiency. This could be justified by the fact that both of the analytes were ionized within the preferred range of the DP pH (NAP ($pK_a \sim 4.2$) and SDF ($pK_a \sim 4$)). Also, there are some limitations for the application of high concentrations of NaOH as the AP such as an increased risk of bubble formation and punctuation in the AP volume. Thus, the pH of the donor and APs were adjusted to 9.6 and 12.3, respectively, for the remaining experiments.

Time and voltage are two important parameters in EME, and the extraction efficiency increases by increasing both of them. Figure 3B depicted that the normalized peak area of drugs increased while increasing the voltage up to 68 V whereas a small decrease was observed at higher voltages. Actually, an average amount of the applied voltage was appropriate for effective extraction; as low voltages could not provide the required driving force, and high voltages led to system instability and bubble formation. Also, results showed (Fig. 3B) that extraction efficiency increased up to 16 min, after which the extraction efficiency decreased. It was assumed that SLM was partly dissolved due to its contact with aqueous solutions on both sides of the hollow fiber. The liquid membrane thickness may decrease for longer extraction times and may not fully separate two aqueous phases. Similar behavior was previously described by Balchen et al. [43].

3.3 Validation of the method

To evaluate the practical applicability of the proposed EME procedure, figures of merit including the linear response function, correlation coefficient (R^2), LODs, LOQs, precision, accuracy, and recovery were investigated. As provided in Table 2 acceptable linear response functions were obtained. The intraday precision (repeatability) of the proposed method, expressed as RSD%, was evaluated by extracting five independent samples spiked at 25 ng/mL and 100 ng/mL with each drug and were found in the range of 4.8–6.7% and 3.0–4.3%, respectively (Table 2). The interday precision (intermediate precision) was investigated by analyzing samples spiked at 25 ng/mL and 100 ng/mL with each drug for three consecutive days and the RSD% values were found in the range of 8.3–10.8% and 5.1–8.4%, respectively (Table 2). The LODs of model compounds, based on a signal to noise (S/N) ratio of 3,

Table 2. Figures of merit of the modified EME method

Analyte	Sample	LOD	LOQ	LRF	R^2	EF	ER (%)	Within-day RSD% ($n = 5$)[a]		Between-day RSD% ($n = 3$)[b]	
								25	100	25	100
NAP	Water	0.1	0.25	0.25-500	0.9994	322	96.5	5.0	3.0	8.3	5.1
	Urine	0.3	1.0	1-500	0.9991	249	74.6	6.5	4.3	10.8	7.0
SDF	Water	0.25	1.0	1-500	0.9998	303	90.8	4.8	3.4	9.2	6.8
	Urine	0.7	2.5	2.5-500	0.9982	238	71.5	6.7	4.0	10.3	8.4

All concentrations are based on ng/mL.
a) *n* is the number of times of sample running.
b) *n* is the number of consecutive days.
LRF, linear response function; R^2, correlation coefficient; ER, extraction recovery.

Table 3. Determination of NAP and SDF in real urine samples

Sample		NAP	SDF
Urine 1	Initial concentration	n.d	n.d
	93.0	RR%[a]	96.5
	RSD% ($n = 3$)	5.5	4.6
Urine 2	Initial concentration	n.d	153[b]
	RR%[a]	105	92.8
	RSD% ($n = 3$)	6.4	4.3
Urine 3	Initial concentration	132[c]	n.d
	RR%[a]	96.0	94.2
	RSD% ($n = 3$)	5.8	7.0

a) Hundred nanogram per milliliters of each drug is added to calculate relative recovery (RR%).
b) Six hours after consumption of a oral dose of 100 mg of SDF.
c) One hundred fifty minutes after consumption of a oral dose of 500 mg of NAP.
n.d, not detected.

were in the 0.1–0.7 ng/mL range while the LOQs (S/N = 10) were in the range of 0.25–2.5 ng/mL (Table 2). The enrichment factor (EF) was defined as the ratio of the final analyte concentration in the AP ($C_{f,a}$) and the initial concentration of analyte in the DP ($C_{i,d}$):

$$EF = \frac{C_{f,a}}{C_{i,d}} \quad (1)$$

Extraction recovery (ER) was calculated according to the following equation for each analyte:

$$ER\,(\%) = \frac{n_{f,a}}{n_{i,d}} \times 100 = \left(\frac{V_a}{V_d}\right)\left(\frac{C_{f,a}}{C_{i,d}}\right) \times 100 \quad (2)$$

where $n_{i,d}$ and $n_{f,a}$ are the number of moles of analyte originally present in the DP and the number of moles of analyte finally collected in the AP, respectively. V_a is the volume of AP and V_d is the volume of DP.

Relative recovery (RR) was acquired from the following equation:

$$RR\,(\%) = \frac{C_{found} - C_{real}}{C_{added}} \times 100 \quad (3)$$

where C_{found}, C_{real}, and C_{added} are the concentration of analyte after the addition of a known amount of the standard into the real sample, the concentration of analyte in real sample, and the concentration of a known amount of standard which was spiked into the real sample, respectively. Also, in order to calculate the EF of each drug, five replicate extractions were performed at optimal conditions from aqueous solution containing 25 ng/mL of each drug. The EF was calculated as the ratio of the final concentration of the analyte in the AP and its concentration in the DP. Good EFs were obtained within the range of 238–322, which corresponds to extraction recoveries of 71.5–96.5% in different samples (Table 2).

3.4 Real sample analysis

To investigate the ER and the applicability of the proposed EME procedure, final experiments were carried out on three real urine samples taken from volunteers (Urine 1, Urine 2, and Urine 3). These urine samples were diluted with pure water (1:1) and their pH values were adjusted at 9.6. Then, 10 mL of each solution was transferred into the sample vial and EME process was applied under the extraction conditions mentioned above. At first, nonspiked urine samples were extracted by EME. The obtained results are illustrated in Table 3. The experimental results revealed that, 153 ng/mL of SDF and 132 ng/mL of NAP were found in Urine 2 and Urine 3, respectively. Then, 100 ng/mL of each drug was added to the real urine samples and extraction procedure was repeated again to calculate relative recoveries. All nonspiked and spiked chromatograms of the real samples are depicted in Fig. 4. The accuracy of the method was determined by analysis of real samples after spiking with proper amounts of standard solution of the drugs. Results of three replicate analyses of each sample obtained are summarized in Table 3. The proposed method shows high relative recoveries for all real samples from 93 to 105%, which ensures the accuracy of the amount of analytes detected in nonspiked real samples.

The present method was compared with other methods in terms of validation and precision (Supporting Information Table 2) [20, 44–51]. The data indicate that the proposed method is efficient, and the sensitivity of the developed method is comparable to or better than that of existing methods for the extraction of the model acidic drugs.

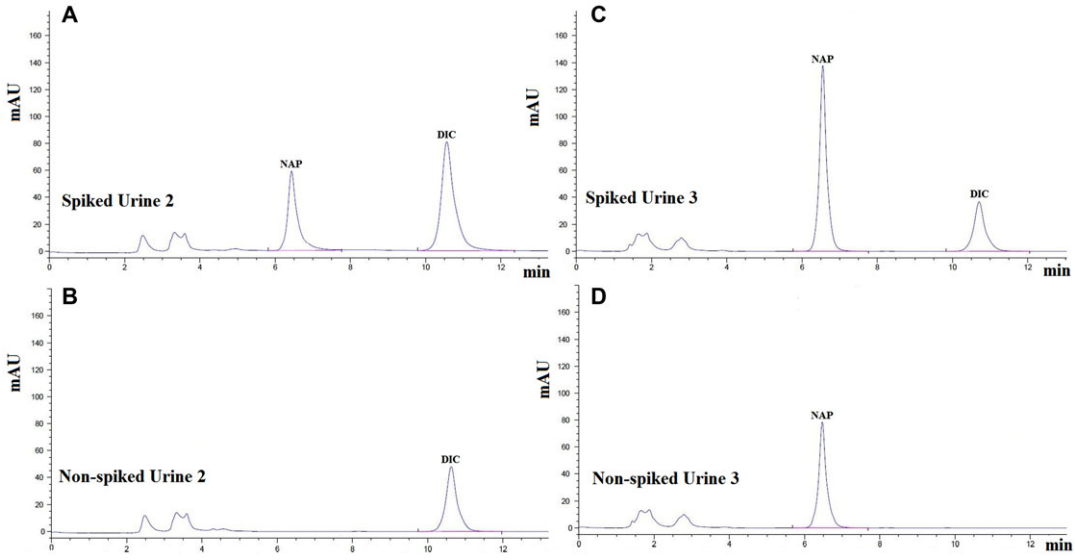

Figure 4. Chromatograms obtained after proposed EME method from (A) Urine 2 sample spiked at a concentration level of 60 ng/mL of each drug, (B) nonspiked Urine 2 sample, (C) Urine 3 sample spiked at a concentration level of 60 ng/mL of each drug, and (D) nonspiked Urine 3 sample. (Extraction condition: HND-G dispersed in 1-octanol (0.6% w/v) as SLM, pH of the AP 12.3, pH of the DP 9.6, 68 V potential difference, 16 min extraction time).

4 Concluding remarks

In this study, for the first time, HND-G was synthesized and then it was successfully applied as a new cationic carrier for the extraction of SDF and NAP as model anionic drugs. Compared to the other G types (G, GO, and ND-G), the immobilization of HND-G in the membrane has been shown to be an effective approach for the enhancement of the EME performance, primarily due to presence of N groups and higher dispersibility of this material. In addition, the ion-pair formation between the acidic drugs with negative charge and HND-G with positive charge at the SLM interface facilitates mass transfer. Also, the results showed that GO had low extraction efficiency due to an electrostatic repulsion between their anionic functional groups with anionic acidic drugs in alkaline media. Considering logical extraction time, as well as satisfactory LOQ, good EF, and also the capability of extraction with low volume of an organic solvent, this type of EME modified with HND-G as cationic carriers may be an interesting future concept for the extraction of many charged analytes.

The authors wish to thank Ferdowsi University of Mashhad, Shahid Beheshti University of Tehran, and University of Birjand for the financial support of this project.

The authors have declared no conflict of interest.

5 References

[1] Lee, J., Lee, H. K., Rasmussen, K. E., Pedersen-Bjergaard, S., *Anal. Chim. Acta* 2008, *624*, 253–268.

[2] Fakhari, A. R., Tabani, H., Nojavan, S., *Drug Test. Anal.* 2013, *5*, 589–595.

[3] Gjelstad, A., Jensen, H., Rasmussen, K. E., Pedersen-Bjergaard, S., *Anal. Chim. Acta* 2012, *742*, 10–16.

[4] Gjelstad, A., Rasmussen, K. E., Pedersen-Bjergaard, S., *J. Chromatogr. A* 2006, *1124*, 29–34.

[5] Pedersen-Bjergaard, S., Rasmussen, K. E., *J. Chromatogr. A* 2006, *1109*, 183–190.

[6] Middelthon-Bruer, T. M., Gjelstad, A., Rasmussen, K. E., Pedersen-Bjergaard, S., *J. Sep. Sci.* 2008, *31*, 753–759.

[7] Gjelstad, A., Rasmussen, K. E., Pedersen-Bjergaard, S., *Anal. Bioanal. Chem.* 2009, *393*, 921–928.

[8] Eibak, L. E. E., Gjelstad, A., Rasmussen, K. E., Pedersen-Bjergaard, S., *J. Chromatogr. A* 2010, *1217*, 5050–5056.

[9] Fakhari, A. R., Tabani, H., Nojavan, S., Abedi, H., *Electrophoresis* 2012, *33*, 506–515.

[10] Seidi, S., Yamini, Y., Saleh, A., Moradi, M., *J. Sep. Sci.* 2011, *34*, 585–593.

[11] Rezazadeh, M., Yamini, Y., Seidi, S., *J. Chromatogr. B* 2011, *879*, 1143–1148.

[12] Tabani, H., Fakhari, A. R., Shahsavani, A., *Electrophoresis* 2013, *34*, 269–276.

[13] Fakhari, A. R., Tabani, H., Behdad, H., Nojavan, S., Taghizadeh, M., *Microchem. J.* 2013, *106*, 186–193.

[14] Ahmar, H., Tabani, H., Koruni, M. H., Davarani, S. S. H., Fakhari, A. R., *Biosens. Bioelectron.* 2014, *54*, 189–194.

[15] Tabani, H., Fakhari, A. R., Shahsavani, A., Behbahani, M., Salarian, M., Bagheri, A., Nojavan, S., *J. Chromatogr. A* 2013, *1300*, 227–235.

[16] Koruni, M. H., Tabani, H., Gharari-Alibabaou, H., Fakhari, A. R., *J. Chromatogr. A* 2014, *1361*, 95–99.

[17] Ramos-Payan, M., Fernandez-Torres, R., Perez-Bernal, J. L., Callejon-Mochon, M., Bello-Lopez, M. A., *Anal. Chim. Acta* 2014, *849*, 7–11.

[18] Sun, J. N., Chen, J., Shi, Y. P., *J. Chromatogr. A* 2014, *1352*, 1–7.

[19] Slampova, A., Kuban, P., Bocek, P., *Electrophoresis* 2014, *35*, 3317–3320.

[20] Hasheminasab, K. S., Fakhari, A. R., Shahsavani, A., Ahmar, H., *J. Chromatogr. A* 2013, *1285*, 1–6.

[21] Hasheminasab, K. S., Fakhari, A. R., *Anal. Chim. Acta* 2013, *767*, 75–80.

[22] Novoselov, K. S., Geim, A. K., Morozov, S. V., Jiang, D., Zhang, Y., Dubonos, S. V., Grigorieva, I. V., Firsov, A. A., *Science* 2004, *306*, 666–669.

[23] Lee, S. U., Belosludov, R. V., Mizuseki, H.; Kawazoe, Y., *Small* 2009, *5*, 1769–1775.

[24] Gong, K., Du, F., Xia, Z., Duratock, M., Dai, L., *Science* 2009, *323*, 760–764.

[25] Hu, S., Wang, A., Li, X., Lowe, H., *J. Phys. Chem. Solids* 2010, *71*, 156–162.

[26] Menezes, H. C., Resende de Barcelos, S. M., Macedo, D. F. D., Purceno, A. D., Machado, B. F., Teixeira, A. P. C., Lago, R. M., Serp, P., Cardeal, Z. L., *Anal. Chim. Acta* 2015, *873*, 51–56.

[27] *United States Pharmacopeia 30-NF 25*, United States Pharmacopeial Convention Inc., Rockville, MD 2007, p. 1922.

[28] Movahed, S. K., Dabiri, M., Bazgir, A., *Appl. Catal. A Gen.* 2014, *488*, 265–274.

[29] Yang, D., Velamakanni, A., Bozoklu, G., Park, S., Stoller, M., Piner, R. D., Stankovich, S., Jung, I., Field, D. A., Ventrice, C. A., *Carbon* 2009, *47*, 145–152.

[30] Jansen, R. J. J., Vanbekkum, H., *Carbon* 1995, *33*, 1021–1027.

[31] Nakayama, Y., Soeda, F., Ishitani, A., *Carbon* 1990, *28*, 21–26.

[32] Jorio, A., Dresselhaus, M. S., Saito R., Dresselhaus, G. F., Wiley-VCH, Berlin 2011.

[33] Fu, X., Bei, F., Wang, X., O'Brien, S., Lombardi J. R. *Nanoscale* 2010, *2*, 1461–1466.

[34] Yang, Z. Y., Zhang, Y. X., Jing, L., Zhao, Y. F., Yan, Y. M., Sun, K. N., *J. Mater. Chem. A* 2014, *2*, 2623–2627.

[35] Hu, H., Zhao, Z., Wan, W., Gogotsi, Y., Qiu, J., *Adv. Mater.* 2013, *25*, 2219–2223.

[36] Wu, P., Qian, Y., Du, P., Zhang, H., Cai, C., *J. Mater. Chem.* 2012, *22*, 6402–6412.

[37] Balchen, M., Gjelstad, A., Rasmussen, K. E., Pedersen-Bjergaard, S., *J. Chromatogr. A* 2007, *1152*, 220–225.

[38] Seip, K. F., Faizi, M., Vergel, C., Gjelstad, A., Pedersen-Bjergaard, S., *Anal. Bioanal. Chem.* 2014, *406*, 2151–2161.

[39] Yamini, Y., Seidi, S., Rezazadeh, M., *Anal. Chim. Acta* 2014, *814*, 1–22.

[40] Yang, S., Feng, X., Ivanovici, S., Müllen, K., *Angew. Chem. Int. Ed.* 2010, *49*, 8408–8411.

[41] Box G. E. P., Behnken DW Some new three level designs for the study of quantitative variables. *Technometrics* 1960, *2*, 455–476.

[42] Jimenez, N., Vinas, M., Bayona, J. M., Albaiges, J., Solanas, A. M., *Appl. Microbiol. Biotechnol.* 2007, *77*, 935–945.

[43] Balchen, M., Halvorsen, T. G., Reubsaet, L., Pedersen-Bjergaard, S., *J. Chromatogr. A* 2009, *1216*, 6900–6905.

[44] Ramos Payan, M., Bello Lopez, M. A., Fernandez-Torres, R., Perez Bernal, J. L., Callejon Mochon, M., *Anal. Chim. Acta* 2009, *653*, 184–190.

[45] Zgola-Grzeskowiak, A., *Chromatographia* 2010, *72*, 672–678.

[46] Sun, Z., Schussler, W., Sengl, M., Niessner, R., Knopp, D., *Anal. Chim. Acta* 2008, *620*, 73–81.

[47] Davarani, S. S. H., Pourahadi, A., Nojavan, S., Banitaba, M. H., Nasiri-Aghdam, M., *Anal. Chim. Acta* 2012, *722*, 55–62.

[48] Ji, Y., Du, Z., Zhang, H., Zhang, Y., *Anal. Methods* 2014, *6*, 7294–7304.

[49] Sarafraz-Yazdi, A., Amiri, A., Rounaghi, G., Eshtiagh-Hosseini, H., *Anal. Chim. Acta* 2012, *720*, 134–141.

[50] Caro, E., Marcé, R. M., Cormack, P. A. G., Sherrington, D. C., Borrull, F., *J. Chromatogr. B* 2004, *813*, 137–143.

[51] Aguilar-Arteaga, K., Rodriguez, J. A., Miranda, J. M., Medina, J., Barrado, E., *Talanta* 2010, *80*, 1152–1157.

